Hindawi Publishing Corporation
International Journal of Distributed Sensor Networks
Volume 2012, Article ID 414692, 12 pages
doi:10.1155/2012/414692

Research Article

Performance Evaluation of PPP-BOTDA-Based Distributed Optical Fiber Sensors

Hao Zhang[1] and Zhishen Wu[2,3]

[1] *School of Civil Engineering, Shijiazhuang Tiedao University, Shijiazhuang, Hebei 050043, China*
[2] *Department of Urban and Civil Engineering, Ibaraki University, Nakanarusawa-cho 4-12-1, Hitachi, Ibaraki 316-8511, Japan*
[3] *International Institute for Urban System Engineering, Southeast University, Nanjing, Jiangsu 210096, China*

Correspondence should be addressed to Hao Zhang, sjzrizh@hotmail.com

Received 30 August 2012; Accepted 16 November 2012

Academic Editor: Jeong-Tae Kim

The basic sensing behaviors of Pulse-Prepump Brillouin Optical Time Domain Analysis- (PPP-BOTDA-) based distributed fiber optic sensors (DFOSs) with a spatial resolution on the order of 0.1 m are first experimentally studied. Second, the sensing results for different types of optical fibres are compared. Based on these investigations, the performance of PPP-BOTDA—based DFOSs for crack monitoring is evaluated. The experimental results show that in the interior of an optical fibre, slippage between the bare fiber and the coating materials occurs and that different types of optical fibres have different degrees of slippage. Point fixation bonding methods can produce effective and correct measurement results when the gauge length of the optical fibre is longer than the critical effective sensing length (CESL), whereas the overall bonding method is still not feasible for monitoring localized deformation quantitatively. Finally, the differences between Brillouin Optical Time Domain Reflectometry (BOTDR) and BOTDA are discussed.

1. Introduction

As a novel and advanced sensing technique, fiber optic sensors (FOSs) have been extensively researched for structural health monitoring (SHM) purpose due to their distributed sensing, rapid data transmission, small dimension, ease of installation, and immunity from electromagnetic influence. Among them, the Brillouin-based sensing is a one type of the most useful and important sensing techniques [1–8]. Investigations on the application of optic fiber sensing techniques for SHM have been widely carried out and significant progress has been made in the recent years [3–14]. In addition to the aforementioned advantages, the Brillouin scattering-based distributed fiber optic sensors show some potential merits over general FOSs for SHM as well, which can be characterized by the following advantages. The optical fiber used as strain sensors can be installed in several and even scores of kilometers. Along the optic fiber, the sampling point can be taken every 5 cm, and thus the strain distribution along the entire length of optical fiber can be obtained in a continuous and distributed way. The sufficient measurement can solve the problem of instability including nonuniqueness and discontinuity of solutions that many damage detection algorithms have encountered. Through the point fixation (PF) installation of the optical fiber, there will be formed a uniform strain distribution between two bonding points, the interval between these two bonding points can vary from scores of centimeters to several meters, and the measured strain is the uniform strain between these two bonding points. Thus, the measured stain is less susceptible to local stress/strain concentration and hence more representative of the entire structural member, which is in favor of monitoring the global behavior of structures.

One of the most applicable approaches for the Brillouin scattering-based distributed optical fiber sensing technology method is the Brillouin Optical Time Domain Reflectometry- (BOTDR-) based technique as demonstrated by Horiguchi et al. and Bao et al. [1–5]. Some investigations

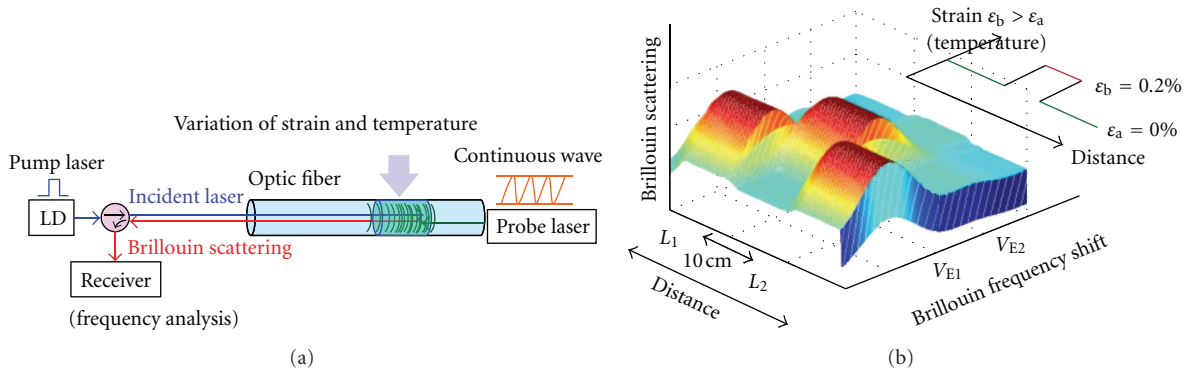

Figure 1: Principle of BOTDA.

on the application of BOTDR techniques for SHM have been carried out [1–6] and significant progress has been made. However, the spatial resolution of BOTDR technique is 1 m with a strain measuring accuracy of $\pm 50\,\mu\varepsilon$. Consequently, the BOTDR sensing technique is difficult to directly monitor the localized deformation (fine crack) of civil structures. In our previous investigation, loop installation of Optical fiber is a good countermeasure [6], but this method is still not convenient for monitoring the practical structure. Recently the newly developed Pulse-Prepump Brillouin Optical Time Domain Analysis (PPP-BOTDA) sensing technique improves largely the spatial resolution (10 cm), and some applications of PPP-BOTDA-based DFOSs for structural health monitoring have been carried out [6, 7].

The improvement in the spatial resolution significantly increases the sensing performance of DFOSs for structural health monitoring. In this paper, to make a good use of this powerful tool, the basic sensing behaviors of PPP-BOTDA-based DFOSs with a spatial resolution on the order of 0.1 m are experimentally studied, and the sensing results from different types of optical fibers are compared. Based on these investigations, the performance of PPP-BOTDA-based DFOSs for crack monitoring is evaluated. Finally, the differences between BOTDR and BOTDA are discussed.

2. PPP-BOTDA-Based Distributed Sensing Technique

2.1. Measurement Principle of BOTDA [8, 9]. The PPP-BOTDA technique is based on stimulated Brillouin backscattering. Two laser sources are introduced into the optic fiber from different ends of the fiber. One is a pulse laser (pump laser) source, and the other is a continuous laser source. When the frequency difference between the two lasers is equal to the Brillouin frequency shift, the Brillouin backscattering will be stimulated and energy transfer will be generated between the two lasers as well, as shown in Figure 1.

The Brillouin frequency shift ν_B changes in proportion to the variation of the strain or temperature, and the linear relationships between the Brillouin frequency shift and the strain or temperature are as follows:

$$\begin{aligned} \nu_B(T_0, \varepsilon) &= C_\varepsilon(\varepsilon - \varepsilon_0) + \nu_{B0}(T_0, \varepsilon_0), \\ \nu_B(T, \varepsilon_0) &= C_T(T - T_0) + \nu_{B0}(T_0, \varepsilon_0), \end{aligned} \tag{1}$$

where C_ε and C_T are the strain and temperature coefficients, respectively, and T_0 and ε_0 are the strain and temperature that correspond to a reference Brillouin frequency ν_{B0}. Spatial information along the fiber length could be obtained through the time-domain analysis by measuring the propagation times for light pulses traveling in the fiber. Thus, continuous temperature and strain distributions along the fiber can be obtained.

2.2. Spatial Resolution. The key to improving the spatial resolution of Brillouin scattering sensing is to shorten the pulse width of the laser pulses. However, for the normal BOTDA sensing technique, when the laser pulse width is shorter than 28 ns, the phonons cannot be fully stimulated, and the stimulated Brillouin gain is also decreased. As a result, the measuring accuracy deteriorates abruptly. To overcome this difficulty, a pre-pump technique has been developed in which two laser sources are introduced into the optical fiber, as shown in Figure 1. The main difference is the pump laser source, which actually includes two types of pulses. One is a prepump laser (PL) that is applied to fully stimulate phonons, and the other is a detection pump (DP) used as a detecting laser. Due to the existence of the PL, the phonons can be fully stimulated before the arrival of the DP. As a result, the pulse width of the DP can be decreased to 1 ns without influencing the stimulation of the Brillouin scattering and the stimulated Brillouin gain. Accordingly, a spatial resolution of approximately 10 cm has recently been realized.

2.3. The Measurement Device. Significant progress has been made in the development of distributed Brillouin scattering-based optic fiber sensors for improving spatial resolution and measurement accuracy and stability. A strain/loss analyser (Neubrexcope-6000, Neubrex Co. Ltd. in Japan.) based on

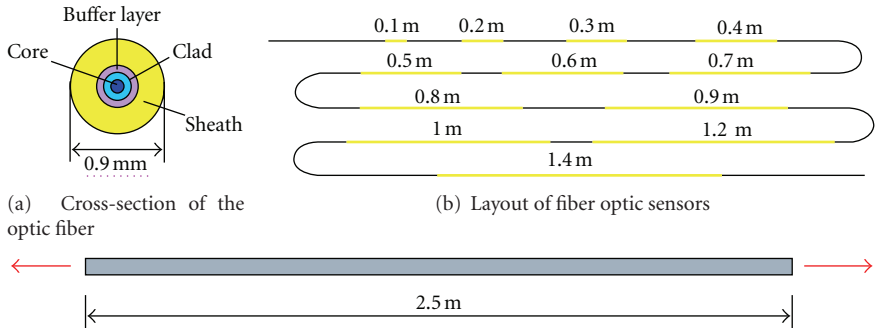

(a) Cross-section of the optic fiber

(b) Layout of fiber optic sensors

(c) Steel specimen.

Figure 2: Measurement behavior of fiber optic sensors.

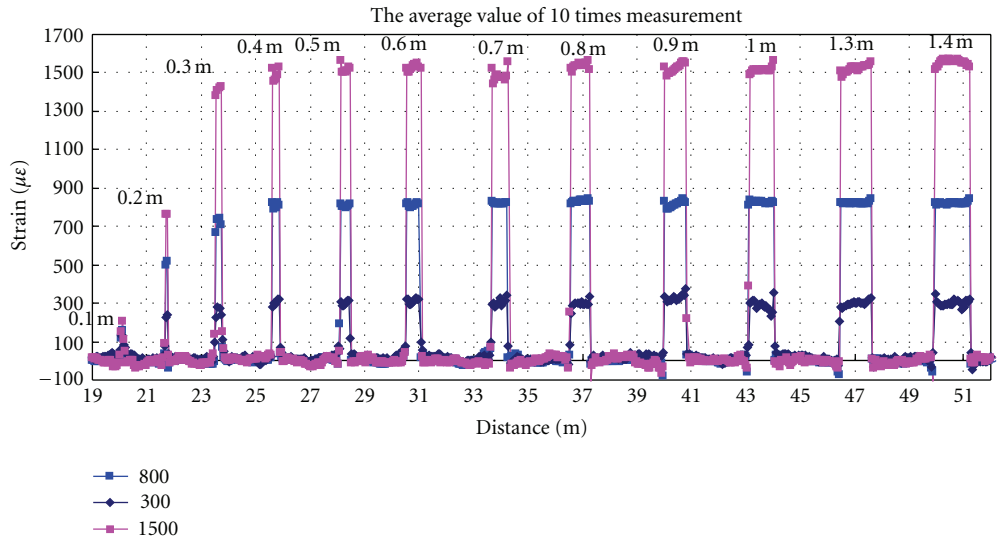

Figure 3: Strain profile along fiber optic sensors.

the PPP-BOTDA technique is used for continuous strain distribution measurement with an optic fiber sensor. Table 1 summarizes the specifications of the Neubrexcope-BOTDA system.

3. Measurement Behavior of Fiber Optic Sensors

The nominal error of the Neubrexcope is $\pm 25\,\mu\varepsilon$, and the minimum spatial resolution of the Neubrexcope is 0.1 m. However, these values are the measured results of non-strained FOSs in a homoisothermal environment. To account for the influence of different factors such as hardware settings, slippage in fiber optic sensors, and fluctuation of the environmental temperature, the actual measurement error may be larger than the nominal value and the measured strain profile will be different from the actual strain profile of the host structure. Therefore, it is necessary to investigate the measured behaviour of BOTDA-based distributed optical fiber sensors experimentally so that the measurement accuracy of BOTDA-based DFOSs can be evaluated.

3.1. Experimental Investigation of the Basic Measurement Behaviour of BOTDA-Based DFOSs. The strain measurement behaviour of FOSs had been examined through basic tests. In an experiment conducted by the authors, 13 segments with different sensing lengths (0.1, 0.2, 0.3, 0.4, 0.5, 0.6, 0.7, 0.8, 0.9, 1.0, 1.2 and 1.4 m) of one piece of optical fiber (type layout of 1; its cross-section is shown in Figure 2(a)) were adhered on the surface of a uniform tensile steel specimen by the overall bonding method. In addition, different sensing segments were separated from each other by an interval of 2 m of free fiber, as shown in Figure 2(b). The applied strain level of the steel specimen was controlled by a strain gauge.

3.2. Measurement Behaviour of a Type 1 Optical Fiber

3.2.1. Strain Profile along a Fiber Optic Sensor. BOTDA monitors the strain profile along the optical fiber with a 5 cm sampling interval. Figure 3 shows the average strain profile of 10 repeated measurements along the whole optical fiber under loading levels of 300, 800, and 1500 $\mu\varepsilon$.

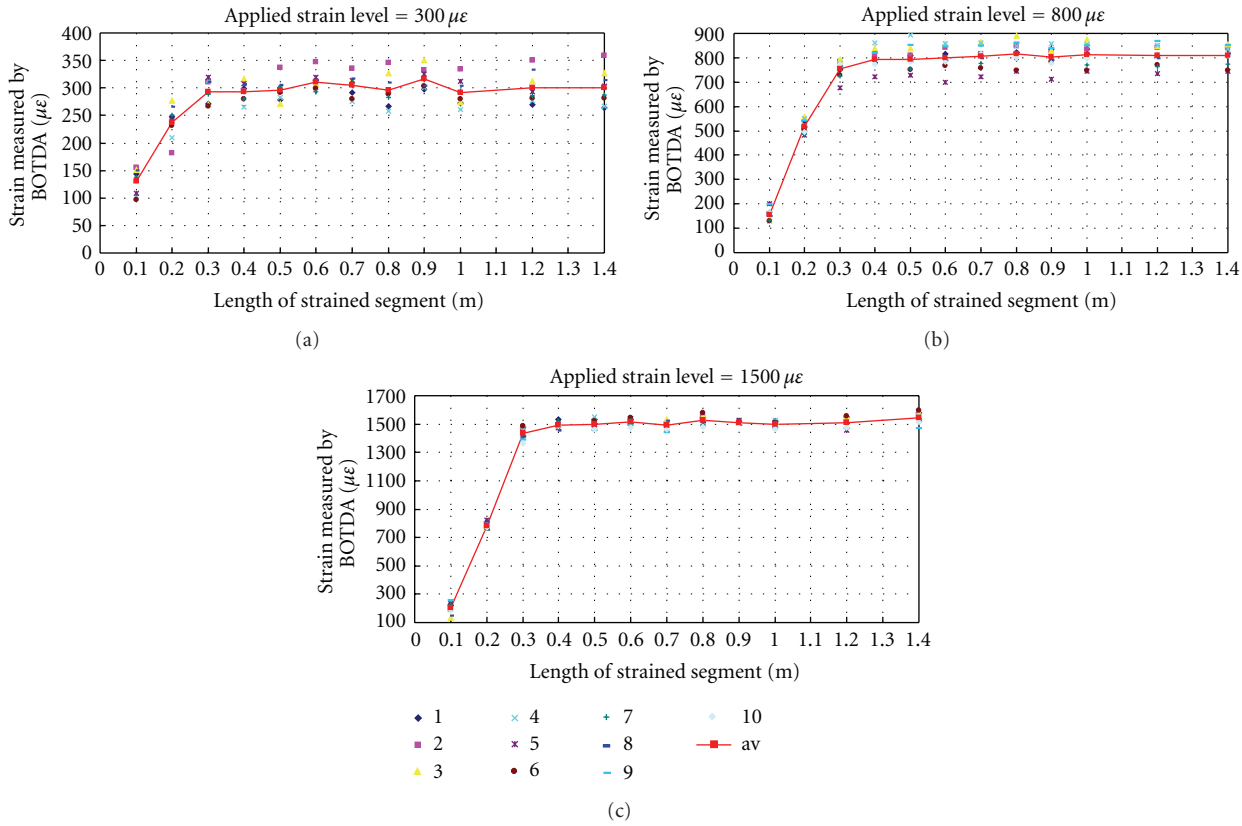

Figure 4: Measurement values of optical fibers with different sensing lengths.

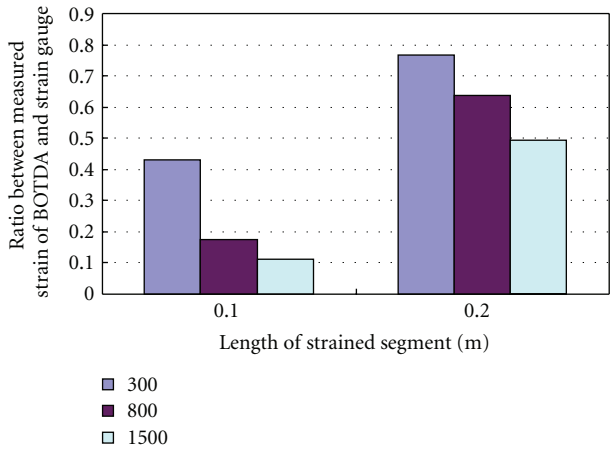

Figure 5: Sensing behaviour of optical fibers.

According to Figure 3, the lengths of the measured strain distributions for different strained FOS segments remain constant at different load levels.

3.2.2. Measurement of the Strain Value of Optical Fibers with Different Sensing Lengths. Under loading levels of 300, 800, and 1500 $\mu\varepsilon$, the 10 measurement strain values of optical fibers with different bonding lengths are shown in Figure 4.

Table 1: Specifications of Neubrexcope systems.

Sampling resolution	5 cm			
Average count	2^5–2^{23} times			
Pulse width (ns)	1	2	5	10
Spatial resolution (m)	0.1	0.2	0.5	1.0
Dynamic range (dB)	1	2	3	5
Max. measurement distance (km)	1	5	10	20
Strain measurement accuracy ($\mu\varepsilon$)	±25	±25	±25	±25
Repeatability ($\mu\varepsilon$)	±50	±50	±50	±50
Temperature test accuracy (°C)	±1	±1	±1	±1

Despite the nominal accuracy of strain measurement is ±25 $\mu\varepsilon$; according to the test results in Figure 4, the maximum difference among 10 times measurements is up to about 100 $\mu\varepsilon$, therefore, in order to monitor actual structure, the strain measurement accuracy of BOTDA needs a substantial increasing.

Based on Figure 4, one important phenomenon should be noted. Despite the spatial resolution of 10 cm (nominal value), if the length of the strained FOS segment is shorter than 0.4 m, the measured strain value of BOTDA is still less than can be detected with the strain gauge. To explain this phenomenon, the strain ratios between the measured BOTDA value and the strain gauge for different load levels are analyzed, as shown in Figure 5.

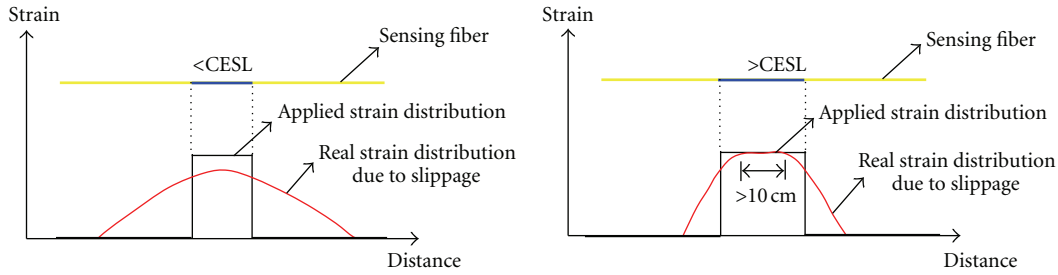

(a) Length of strained segment less than the CESL (b) Length of strained segment less than the CESL

Figure 6: Strain redistribution in FOS.

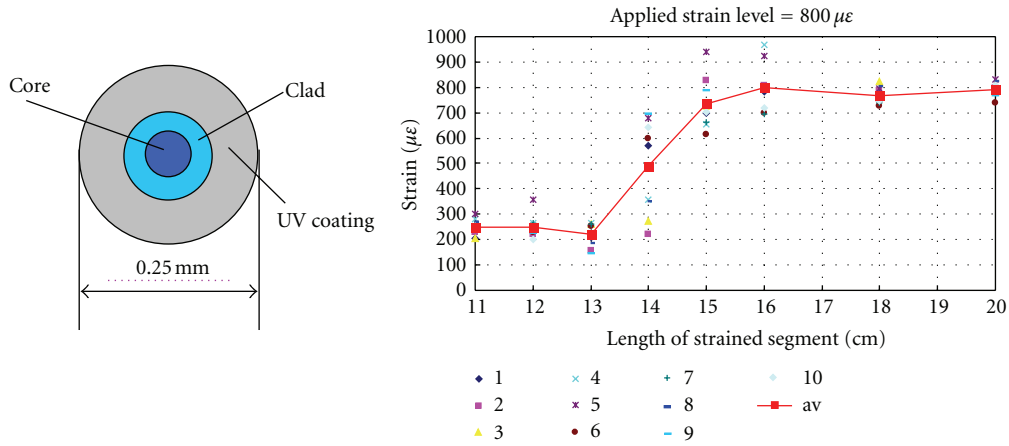

(a) (b)

Figure 7: Sensing behaviour of the optical fiber (type 2).

According to Figure 5, the larger the applied strain, the smaller the strain ratio of the measured value of BOTDA and the strain gauge. Therefore, slippage between the bare fiber and the coating materials may occur. Subsequently, the strain in optical fibers will redistribute, as shown in Figure 6(a), and this strain redistribution lowers the measured strain of BOTDA and results in a measured value of BOTDA below the correct value. At present, the detailed strain distribution of FOS still remains an unresolved problem. Nevertheless, based on the aforementioned analysis, to obtain the correct measured value by using this type of FOS, the length of the strained FOS should be longer than 0.4 m. This length is defined as the critical effective sensing length (CESL).

If the length of the strained FOS segment is longer than the CESL, after strain redistribution caused by slippage, there still exists upwards of 10 cm (spatial resolution) of uniform strain distribution whose value equals the applied strain value to ensure that the BOTDA system can obtain a correct measurement, as shown in Figure 6(b).

3.3. Measurement Behaviour of a Type 2 Optical Fiber. To check the internal slippage of the FOS, another type of optical fiber (as shown in Figure 7) was adhered to the same tensile steel specimen, and the same experimental procedure was performed. Eight segments with different lengths (0.1 m–0.16 m, 0.18 m, and 0.2 m) are set in series. Under a loading level of 800 $\mu\varepsilon$, the 10 measured strain values of the different strained FOS segments are shown in Figure 7.

According to Figure 7, if the length of the strained segment is longer than 0.16 m, the error associated with the measurement is smaller than 40 $\mu\varepsilon$ (5% of the applied strain level), and the measurements of BOTDA are close to the correct value. Obviously, the CESL of a type 2 FOS is 16 cm.

3.4. Measurement Behaviour of a Bare Optical Fiber

3.4.1. CESL of a Bare Fiber. For an FOS, if the length of the strained segment of the FOS is shorter than the CESL, the measured strain of BOTDA is less than that of the strain gauge. The actual spatial resolution of BOTDA is greater than 10 cm, which needs to be investigated further. To completely prevent slippage of the FOS, the UV coating of the type 2 FOS is peeled away, and the bare optic fiber is used to directly carry out the same experiment. The experimental results are illustrated in Figure 8.

From the experimental results depicted graphically in Figure 8, if the sensing length of the bare FOS is longer than 13 cm, BOTDA can produce the correct measurement. Thus,

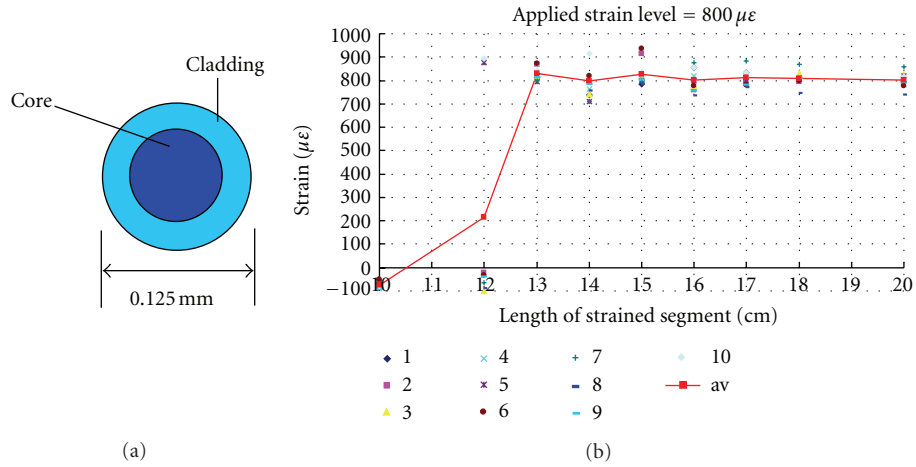

Figure 8: Sensing behaviour of the optical fiber (bare fiber).

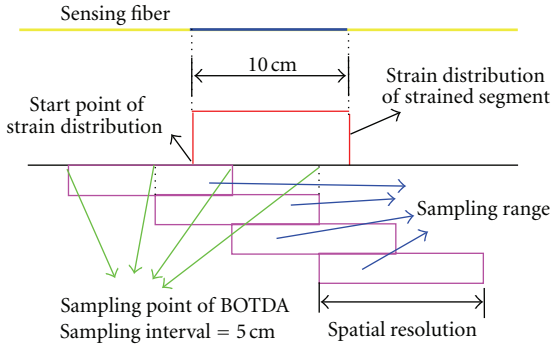

Figure 9: Gap between the sampling point and the starting point of the strained fiber.

the CESL of a bare optical fiber can be considered to be 13 cm.

When the length of the strained segment is only 0.1 m, the measurement is exceptionally undervalued, which can be explained. During the measurement, the sampling interval of PPP-BOTDA is 5 cm; generally, the 0.1 m uniform strain distribution is rarely considered exactly within a certain sampling point measurement by the PPP-BOTDA with a 0.1 m spatial resolution. There is a gap between the sampling point of BOTDA and the starting point of the strained segment, as shown in Figure 9. The range of the gap is considered to be from 0 to 2.5 cm. Thus, only the length of the strained bare FOS is longer than 0.125 m, to ensure that at least one sampling point can measure a 10 cm completely uniform strain distribution, and this sampling point can obtain the correct measured value. Therefore, the PPP-BOTDA sensing technique has a spatial resolution on the order of 10 cm.

Based on the aforementioned experimental result, different types of FOSs have different CESLs, and the CESL parameter can be used to evaluate the anti-slippage property of FOSs. Obviously, if the FOS has a worse anti-slippage property, the deformation of the strained segment will extend into the range of the adjacent non-strained FOSs. To measure a uniform strain distribution whose value equals the applied strain and is more than 10 cm in length (spatial resolution), the longer strained length is necessary so that the BOTDA system can obtain the correct measurement. Therefore, the longer the CESL is, the worse the anti-slippage property becomes [7].

3.4.2. Measurement Behaviour of BOTDA When the Strained Length of FOS Is Less Than the Spatial Resolution. In our previous investigation on BOTDR [6], when the strained length of FOS is less than the spatial resolution (1 m), the BOTDR device can obtain certain strain values. This characteristic can improve the ability of BOTDR to monitor localized deformation. In this section, an experiment similar to that described in Section 3.1 is used to investigate the measurement behaviour of BOTDA in the case in which the strained length of the FOS is less than the spatial resolution. A bare optical fiber is used in this experiment. The measured results are illustrated in Figure 10.

Based on the experimental results, at different load levels when the strained length of the FOS is less than the spatial resolution, the measured results of BOTDA are close to 0 and there is a large variance among the 10 repeated measurements. Consequently, if no internal slippage occurs, the BOTDA system is not able to directly monitor localized deformation whose strained range is less than the spatial resolution.

4. Performance Evaluation of PPP-BOTDA for Crack Monitoring

4.1. Test Method

4.1.1. Specimen. In this study, standard experiments are proposed to calibrate the crack measurement performance of the BOTDA-based distributed optical fiber sensors and to evaluate the accuracy of the measurement. The schematic illustration of the applied standard specimen is shown in

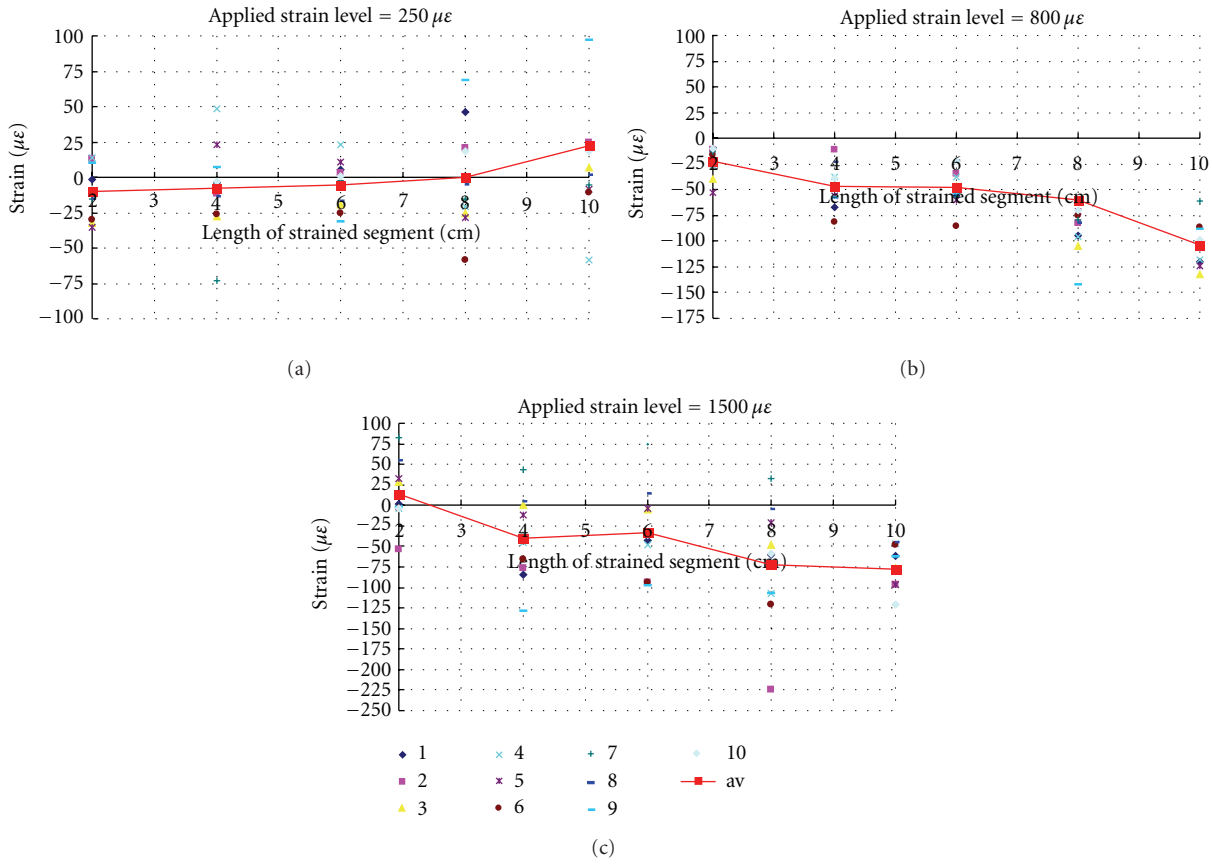

Figure 10: Strain redistribution in the FOS.

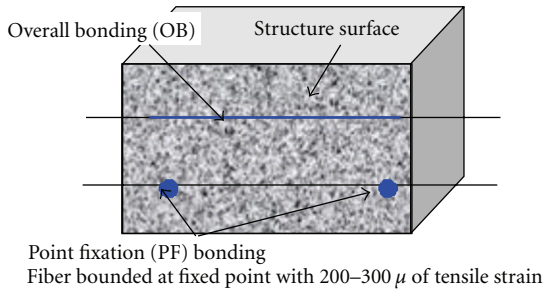

Figure 11: OB and PF installation of the FOS.

Figure 12(a). Two rectangular concrete blocks are connected with two strips of FRP sheets, and the small gap between the two blocks is utilized to simulate an ideal concrete crack. The specimen is axially loaded under a load control mode. Upon loading, the gap becomes wider, and its width is measured by BOTDA-based DFOSs. Simultaneously, the width of the gap is measured by means of displacement transducers (DTs) for comparison.

4.1.2. Bonding Method of the FOS. For different measurement purposes, two installation methods for attaching the optic fiber sensor to the surface of the specimen are proposed and studied. One is termed the overall bonding (OB) method. In the OB method, the necessary measured length of the fiber optic is bonded completely to the surface of the specimen with resin. The OB method is suitable for monitoring strain distribution over a large area. The second installation method is termed the point fixation (PF) bonding method. In the PF bonding method, the two ends of the fiber optic sensor are bonded to the specimen to form a uniform strain distribution within the two bonding points. The measured value of this uniform strain distribution area can be regarded as an average strain value of the gauge length. Consequently, if the gauge length is longer than the spatial resolution, the PF-installed FOS can be effectively used to monitor and measure the crack width of civil engineering structures. Figure 11 schematically demonstrates the OB and PF installation.

4.1.3. Placement of the FOS. In the experiment carried out by the author, the two types of optical fiber described previously were used. For the type 1 optical fiber, the gauge lengths of the PF bonding method are 0.2 m, 0.3 m, and 0.4 m, respectively, and for the type 2 optical fiber, the gauge lengths for the point fixation bonding method are 0.1 m, 0.15 m, 0.2 m, and 0.3 m, respectively (Figure 12).

4.2. Performance Assessment. To assess the performance of BOTDA for crack monitoring, the measured DT data are

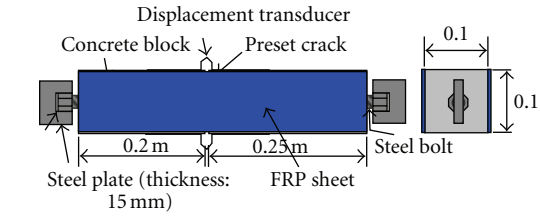

(a) Side view

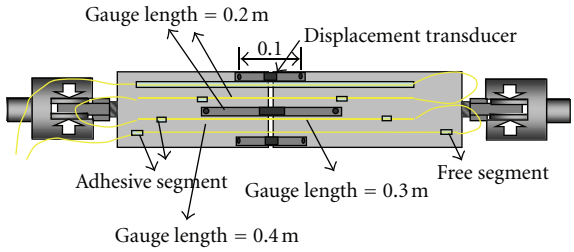

(b) Layout of optic fiber (type 1)

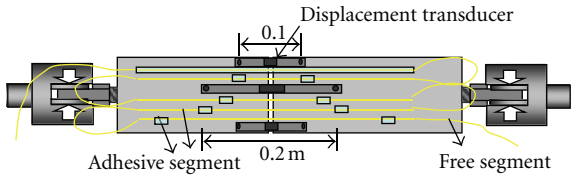

(c) Layout of optical fiber (type 2)

Figure 12: Experiment specimens.

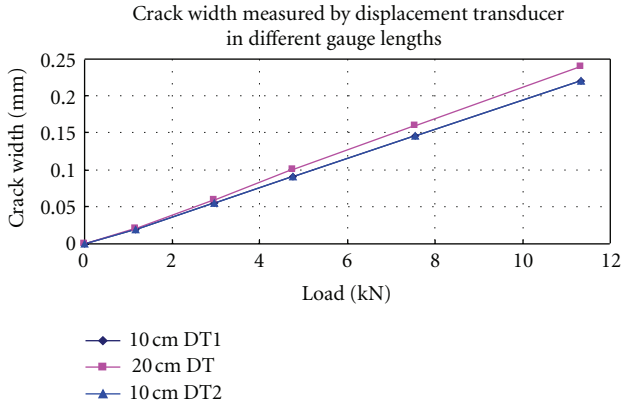

Figure 13: DT measurement results.

used as a baseline to check the accuracy of BOTDA. The measured DT results for different gauge lengths and different load levels are shown in Figure 13.

According to Figure 13, two DTs whose gauge lengths are equal to 10 cm give almost the same measured value, and the measured values of the DTs whose gauge lengths equal 20 cm are bigger than the DTs whose gauge lengths equal 10 cm. Thus, this type of deformation can be used to simulate an ideal concrete crack while taking the elastic deformation of concrete block into consideration. The strain on the surface of a concrete structure can be expressed by the following equation:

$$\varepsilon = \frac{\Delta}{l} = \frac{\Delta_{cr} + \Delta_c}{l}, \quad (2)$$

where Δ_{cr} is the simulated crack width, Δ_c is the deformation of concrete, and l is the gauge length.

According to Figure 12, the total deformation over the gauge length of 0.1 m, 0.15 m, 0.2 m, 0.3 m, and 0.4 m can be calculated. Moreover, these deformations over different gauge lengths can be converted to the corresponding strain values and then used to check the test accuracy of BOTDA.

4.2.1. Assessment of the PF Bonding Method. The measured results of type 1 FOS are shown in Figure 14.

With reference to Figure 14, for type 1 optical fiber with a gauge length less than 0.4 m, the measured strain value of BOTDA is smaller than the converted strain of DT; the smaller the gauge length is, the smaller the ratio of the measured strain of BOTDA to the converted strain of the DT becomes. The conclusion for Section 3.2.2 is also applicable here. However, the PF bonding method can only provide the total deformation over the gauge length; the exact position of cracks and the number of cracks cannot be adequately identified.

The measured results for type 2 optical fiber are shown in Figure 15.

Based on Figure 15, if the sensing length of the type 2 optical fiber is longer than 0.2 cm and the measurement of BOTDA agrees with the DT very well, the CESL of the type 2 optical fiber should be longer than 10 cm and less than 20 cm. This conclusion is practically the same as that of Section 3.3.

4.2.2. Assessment of the OB Method. The measured results of the two types of FOSs applied with the OB bonding method are illustrated in Figure 16.

According to Figure 16, for a preset crack width of 0.6 cm (a value much less than the 10 cm spatial resolution), the overall bonding method can reflect the propagation of the crack. Because the sensing region of the optical fiber sensor is bonded completely to the surface of the specimen with epoxy resin, the strain distribution generated in the concrete is thus directly given by the bonded optical fiber. For any occurrence of and propagation of cracks in concrete structures, there must be a debonding between the epoxy resin and the cracked concrete surface, with localized strain occurring on the fiber close to both sides of the crack, as shown in Figure 17(a). In the case of perfect bonding, the fiber would never survive such a large localized strain. Except for the slippage between the optic fiber and the epoxy resin, the optical fiber located at the cracked position is strained and elongated. Moreover, this localized strain peak also causes internal slippage of the optical fiber, and the localized strain peak is distributed near the optical fiber segment. Consequently, the strain distribution of the sensing fiber should be similar to Figure 17(b). However, performing detailed strain measurements close to cracks is still an unresolved problem, and no stable relationship is

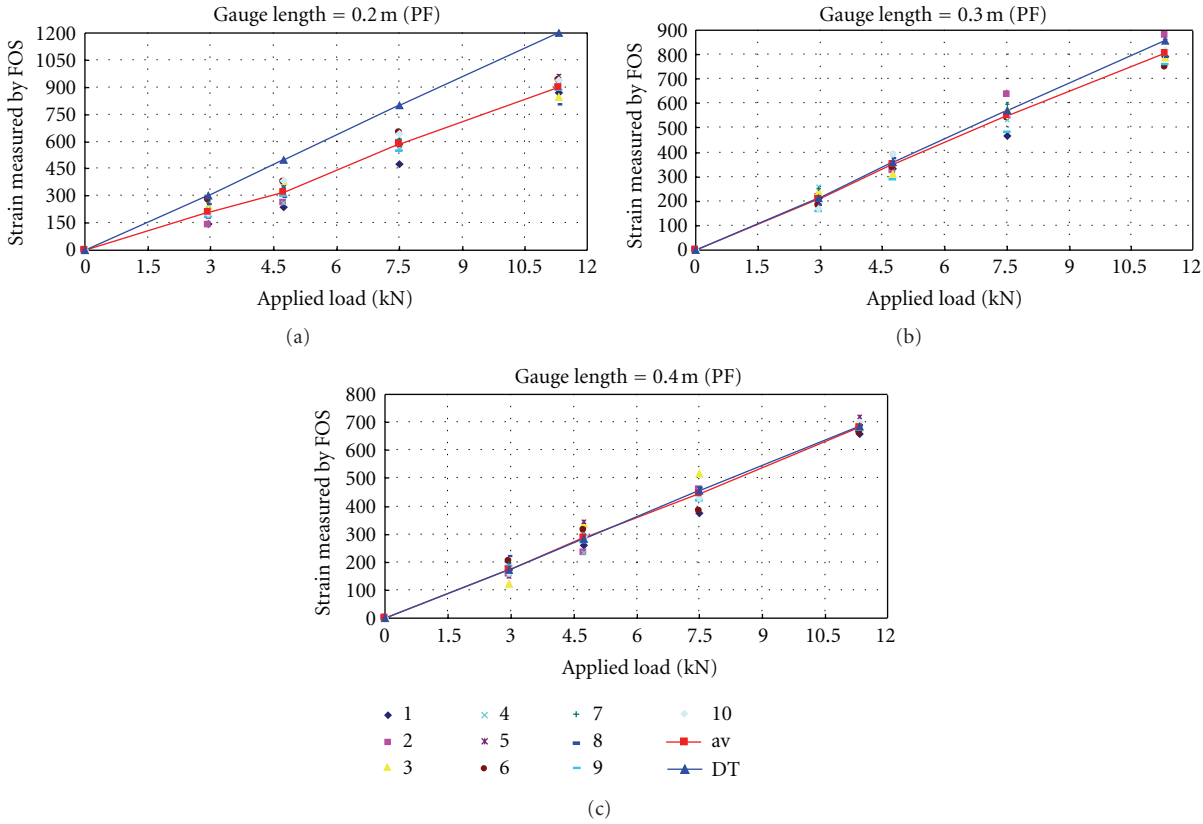

Figure 14: Measurement results for the optical fiber (type 1).

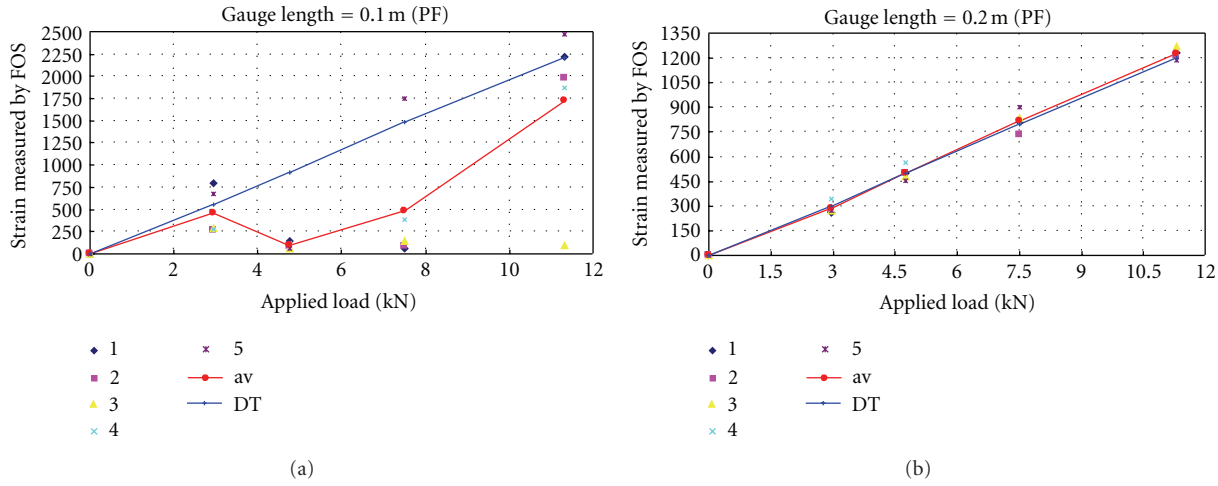

Figure 15: Measurement result for the optical fiber (type 2).

found between the measured strain from the overall bonding and the converted strain of the DT. Thus, the overall bonding method is still not feasible for monitoring the crack width quantitatively.

According to Figure 17, for a type 2 FOS, because of the good antislippage property, the measured result for the optic fiber installed with the overall bonding method is much smaller than that for type 1 FOS. Thus, for the overall bonding method, the slippage of the FOS is favorable to monitor cracking of the concrete structure. If slippage of the FOS can be completely prevented, the overall bonding method may lead to the rupture of optic fibers and hence lose its ability to reflect the existence of cracks.

5. Comparisons with BOTDR

In our previous investigation [6], the measurement behaviour of BOTDR was discussed and the performance

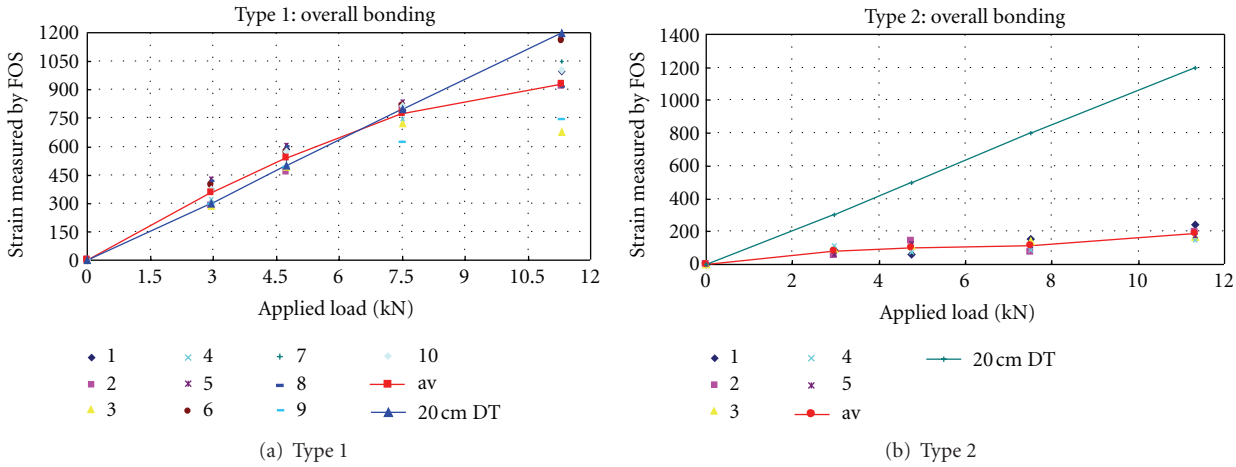

(a) Type 1 (b) Type 2

Figure 16: Measurement result for an optical fiber installed by the overall bonding method.

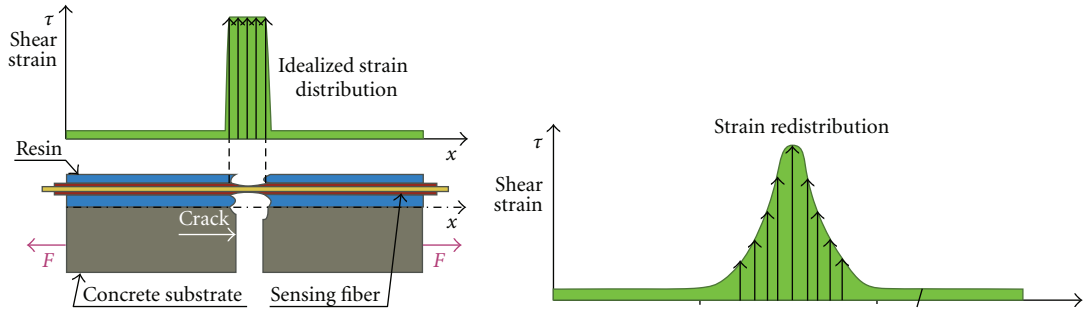

(a) (b)

Figure 17: Strain redistribution in optical fibers.

of BOTDR for crack monitoring was evaluated with the same experiment. The PPP-BOTDA sensing technique has a significantly improved spatial resolution; therefore, it is necessary to compare these two distributed fiber optic sensing techniques.

5.1. Monitoring Localized Deformation. The nominal spatial resolutions of BOTDR and PPP-BOTDA are 1 m and 0.1 m, respectively. The improvement in the spatial resolution is good for detecting the localized deformation. For the BOTDA technique, an optical fiber installed with the PF method can be used to monitor cracking or localized deformation. For the BOTDR technique, the optic fiber should be installed with the loop installation method.

5.2. Relation of Truly Measured Strain Distributed Range and Actual Strain Distributed Range (Sensing Length). For the BOTDR technique, the length of the actual strain distribution can be calculated from the length of the measured strain distribution by using the following equation [6]:

$$l = L_t - L, \tag{3}$$

where l is the length of the truly measured strain distribution, and L is the spatial resolution, L_t: the length of the actual strain distribution.

The correctness of (3) was verified by our experiments which are similar as the experiments carried out in Section 3.1. The actual length of the fiber optic sensor installed in the point fixation method is 1.4 m. According to (3), the truly measured length of the optic fiber can be calculated: $l = L_t - 1 = 0.4$ m, which agrees with the experimental result (0.45 m), as shown in Figure 18.

For the BOTDA technique, based on the experimental result of Section 3.2, the length of the actual strain distribution also can be calculated from the length of the truly measured strain distribution by using (3); consequently, the truly measured length of optic fiber can be calculated: $l = L_t - 1 = 1.3$ m, which agrees with the experimental result, as shown in Figure 19.

6. Conclusions

(1) Based on the experimental results for the bare fiber, the PPP-BOTDA sensing technique has a 10 cm spatial resolution.

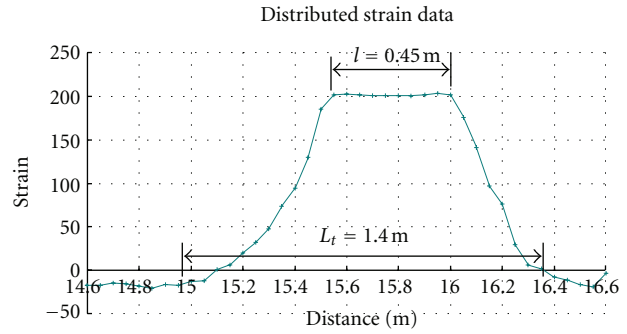

Figure 18: Distributed strain data along an optic fiber measured by BOTDR (sensing length = 1.4 m).

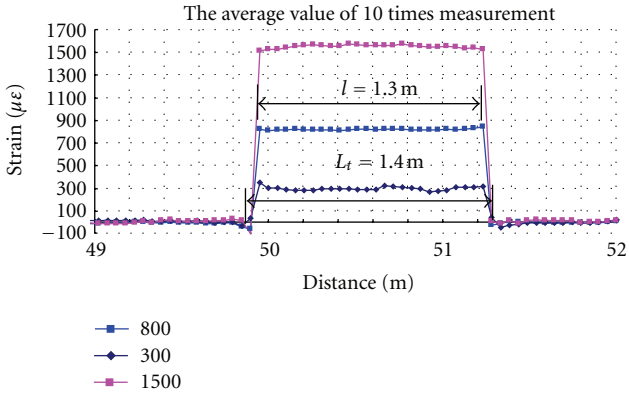

Figure 19: Distributed strain data along an optic fiber measured by BOTDA (sensing length = 1.4 m).

(2) Despite the 10 cm spatial resolution, if the sensing length of the FOS is less than the CESL because of slippage between the bare fiber and the coating materials of the optic fiber, the BOTDA measurement result will not be correct. Different types of FOSs have different CESLs, and the longer the CESL is, the worse the antislippage property becomes.

(3) Point fixation installation methods can give effective and correct measurement results for monitoring localized deformation when the gauge length of the optical fiber is longer than the CESL.

(4) The overall bonding method can reflect the existence of cracking or localized deformation, but it is still unfit for monitoring crack width quantitatively.

(5) A higher number of repeated measurement counts and smaller scanning steps can improve the measurement accuracy, but these settings can increase the measurement time significantly.

(6) An effective way to reduce the error level of BOTDA is to adopt the average values of several time measurements.

Acknowledgment

The authors would like to thank there viewers for their detailed comments that have helped to improve the quality of the paper. This work is supported by the Major Programs of the Chinese Academy of Sciences during the 12th Five-Year Plan Period (no. 2011BAK02B03); the National Natural Science Foundation of China (no. 51208113); Natural Science Foundation of Hebei Province of China (no. E2013210); The Foundation for Development of Science and Technology of Fuzhou University (no. 2012-XQ-33).

References

[1] T. Horiguchi, T. Kurashima, and M. Tateda, "Tensile strain dependence of Brillouin frequency shift in silica optical fibers," *IEEE Photonics Technology Letters*, vol. 1, no. 5, pp. 107–108, 1989.

[2] T. Kurashima, T. Horiguchi, H. Izumita, S. I. Furukawa, and Y. Koyamada, "Brillouin optical-fiber time domain reflectometry," *IEICE Transactions on Communications*, vol. E76-B, no. 4, pp. 382–390, 2002.

[3] X. Bao, M. DeMerchant, A. Brown, and T. Brenner, "Strain measurement of the steel beam with the distributed Brillouin scattering sensor," in *Health Monitoring and Management of Civil Infrastructure Systems*, vol. 4337 of *Proceedings of SPIE*, pp. 223–233, Newport Beach, Calif, USA, March 2001.

[4] X. Bao, D. J. Webb, and D. A. Jackson, "Distributed temperature sensor based on Brillouin loss in an optical fibre for transient threshold monitoring," *Canadian Journal of Physics*, vol. 74, no. 1-2, pp. 1–3, 1996.

[5] X. Gu, Z. Chen, and F. Ansari, "Embedded fiber optic crack sensor for reinforced concrete structures," *ACI Structural Journal*, vol. 97, no. 3, pp. 468–476, 2000.

[6] Z. Hao and W. Zhishen, "Performance evaluation of BOTDR-based distributed fiber optic sensors for crack monitoring," *Structural Health Monitoring*, vol. 7, no. 2, pp. 143–156, 2008.

[7] W. Zhishen, I. Kentaro, X. Songtao, and Z. Hao, "Experimental Study on Crack Monitoring of PC structures with pulse-prepump BOTDA-based distributed fiber optic sensors," *Journal of Concrete Research and Technology, Japan Concrete Institute*, vol. 18, no. 2, 2007.

[8] K. Kishida and C.-H. Li, "Pulse pre-pump-BOTDA technology for new generation of distributed strain measuring system," in *Structural Health Monitoring and Intelligent Infrastructure*, Ou, Li, and Daun, Eds., pp. 471–477, Taylor & Francis, 2006.

[9] K. Kishida, L. Che-Hien, and K. Nishiguchi, "Pulse pre-pump method for cm-order spatial resolution of BOTDA," in *Proceedings of the 17th International Conference on Optical Fibre Sensors (OFS '05)*, SPIE, pp. 559–562, May 2005.

[10] L. Suzhen and W. Zhishen, "Structural identification using static macro-strian measurements from long-gauge fiber optic sensors," *Journal of Applied Mechanics*, vol. 8, pp. 943–948, 2005.

[11] K. Peters, P. Pattis, J. Botsis, and P. Giaccari, "Experimental verification of response of embedded optical fiber Bragg grating sensors in non-homogeneous strain fields," *Optics and Lasers in Engineering*, vol. 33, no. 2, pp. 107–119, 2000.

[12] W. Zhishen and Z. Hao, "A standard test method for evaluating crack monitoring performance of distributed fiber optic sensors," in *Proceeding of the 3rd International Conference on Structural Health Monitoring of Intelligent Infrastructure*, Vancouver, Canada, 2007.

[13] H. Zhang and Z. Wu, "Performance evaluation of BOTDA based distributed optic fiber sensors for crack monitoring," Proceedings of the Japan Concrete Institute, Technical Paper, 2007.

[14] I. -B. Kwon, "Distributed measurements of structures by fiber optic sensors," *Structural Engineering*, vol. 7, no. 6, pp. 659–666, 2003.